



4-15-2015

## Regulation of the Stem Cell–Host Immune System Interplay Using Hydrogel Coencapsulation System with an Anti-Inflammatory Drug

Alireza Moshaverinia

Chider Chen  
*University of Pennsylvania*

Xingtian Xu

Sahar Ansari

Homayoun H. Zadeh

*See next page for additional authors*

Follow this and additional works at: [https://repository.upenn.edu/dental\\_papers](https://repository.upenn.edu/dental_papers)

 Part of the [Dentistry Commons](#)

---

### Recommended Citation

Moshaverinia, A., Chen, C., Xu, X., Ansari, S., Zadeh, H. H., Schrickler, S. R., Paine, M. L., Moradian-Oldak, J., Khademhosseini, A., Snead, M. L., & Shi, S. (2015). Regulation of the Stem Cell–Host Immune System Interplay Using Hydrogel Coencapsulation System with an Anti-Inflammatory Drug. *Advanced Functional Materials*, 25 (15), 2296-2307. <http://dx.doi.org/10.1002/adfm.201500055>

This paper is posted at ScholarlyCommons. [https://repository.upenn.edu/dental\\_papers/123](https://repository.upenn.edu/dental_papers/123)  
For more information, please contact [repository@pobox.upenn.edu](mailto:repository@pobox.upenn.edu).

---

## Regulation of the Stem Cell–Host Immune System Interplay Using Hydrogel Coencapsulation System with an Anti-Inflammatory Drug

### Abstract

The host immune system is known to influence mesenchymal stem cell (MSC)-mediated bone tissue regeneration. However, the therapeutic capacity of hydrogel biomaterial to modulate the interplay between MSCs and T-lymphocytes is unknown. Here it is shown that encapsulating hydrogel affects this interplay when used to encapsulate MSCs for implantation by hindering the penetration of pro-inflammatory cells and/or cytokines, leading to improved viability of the encapsulated MSCs. This combats the effects of the host pro-inflammatory T-lymphocyte-induced nuclear factor kappaB pathway, which can reduce MSC viability through the CASPASE-3 and CAS-PASE-8 associated proapoptotic cascade, resulting in the apoptosis of MSCs. To corroborate rescue of engrafted MSCs from the insult of the host immune system, the incorporation of the anti-inflammatory drug indomethacin into the encapsulating alginate hydrogel further regulates the local microenvironment and prevents pro-inflammatory cytokine-induced apoptosis. These findings suggest that the encapsulating hydrogel can regulate the MSC-host immune cell interplay and direct the fate of the implanted MSCs, leading to enhanced tissue regeneration.

### Disciplines

Dentistry

### Author(s)

Alireza Moshaverinia, Chider Chen, Xingtian Xu, Sahar Ansari, Homayoun H. Zadeh, Scott R. Schrickler, Michael L. Paine, Janet Moradian-Oldak, Ali Khademhosseini, Malcolm L. Snead, and Songtao Shi



Published in final edited form as:

*Adv Funct Mater.* 2015 April 15; 25(15): 2296–2307. doi:10.1002/adfm.201500055.

## Regulation of the Stem Cell–Host Immune System Interplay Using Hydrogel Coencapsulation System with an Anti-Inflammatory Drug

**Dr. Alireza Moshaverinia,**

Center for Craniofacial Molecular Biology (CCMB), Ostrow School of Dentistry, University of Southern California, 2250 Alcazar St, Los Angeles, CA 90033, USA

**Dr. Chider Chen,**

School of Dental Medicine, University of Pennsylvania, 240 South 40th Street, Philadelphia, PA 19104, USA

**Dr. Xingtian Xu,**

Center for Craniofacial Molecular Biology (CCMB), Ostrow School of Dentistry, University of Southern California, 2250 Alcazar St, Los Angeles, CA 90033, USA

**Dr. Sahar Ansari,**

Center for Craniofacial Molecular Biology (CCMB), Ostrow School of Dentistry, University of Southern California, 2250 Alcazar St, Los Angeles, CA 90033, USA

**Dr. Homayoun H. Zadeh,**

Center for Craniofacial Molecular Biology (CCMB), Ostrow School of Dentistry, University of Southern California, 2250 Alcazar St, Los Angeles, CA 90033, USA

**Dr. Scott R. Schricker,**

College of Dentistry, Ohio State University, 305 W 12th Ave, Columbus, OH 43210, USA

**Prof. Michael L. Paine,**

Center for Craniofacial Molecular Biology (CCMB), Ostrow School of Dentistry, University of Southern California, 2250 Alcazar St, Los Angeles, CA 90033, USA

**Prof. Janet Moradian-Oldak,**

Center for Craniofacial Molecular Biology (CCMB), Ostrow School of Dentistry, University of Southern California, 2250 Alcazar St, Los Angeles, CA 90033, USA

**Prof. Ali Khademhosseini,**

Biomaterials Innovation Research Center Harvard Medical School 65 Landsdowne St, Rm 252, Cambridge, MA 02139, USA

**Prof. Malcolm L. Snead, and**

Center for Craniofacial Molecular Biology (CCMB), Ostrow School of Dentistry, University of Southern California, 2250 Alcazar St, Los Angeles, CA 90033, USA

---

Correspondence to: Alireza Moshaverinia, moshaver@usc.edu; Songtao Shi, songtaos@dent1.upenn.edu.

### Supporting Information

Supporting Information is available from the Wiley Online Library or from the author.

**Prof. Songtao Shi**

School of Dental Medicine, University of Pennsylvania, 240 South 40th Street, Philadelphia, PA 19104, USA

Alireza Moshaverinia: moshaver@usc.edu; Songtao Shi: songtaos@dental.upenn.edu

**Abstract**

The host immune system is known to influence mesenchymal stem cell (MSC)-mediated bone tissue regeneration. However, the therapeutic capacity of hydrogel biomaterial to modulate the interplay between MSCs and T-lymphocytes is unknown. Here it is shown that encapsulating hydrogel affects this interplay when used to encapsulate MSCs for implantation by hindering the penetration of pro-inflammatory cells and/or cytokines, leading to improved viability of the encapsulated MSCs. This combats the effects of the host pro-inflammatory T-lymphocyte-induced nuclear factor kappaB pathway, which can reduce MSC viability through the CASPASE-3 and CAS-PASE-8 associated proapoptotic cascade, resulting in the apoptosis of MSCs. To corroborate rescue of engrafted MSCs from the insult of the host immune system, the incorporation of the anti-inflammatory drug indomethacin into the encapsulating alginate hydrogel further regulates the local microenvironment and prevents pro-inflammatory cytokine-induced apoptosis. These findings suggest that the encapsulating hydrogel can regulate the MSC-host immune cell interplay and direct the fate of the implanted MSCs, leading to enhanced tissue regeneration.

**1. Introduction**

Repair and regeneration of craniofacial bone defects have been widely achieved with bone grafting procedures.<sup>[1-3]</sup> However, several disadvantages are associated with this treatment modality,<sup>[4-7]</sup> making bone regeneration using mesenchymal stem cells (MSCs) an advantageous alternative therapeutic option.<sup>[4-6]</sup>

Biomaterials have been utilized to control and manipulate the fate of stem cells leading to high quality tissue regeneration.<sup>[9,10]</sup> However, controlling the fate of the transplanted stem cells is still a major challenge. Biomaterial-MSC interactions have largely been studied by encapsulating the cells within hydrogel biomaterials.<sup>[11,12]</sup> In bone tissue engineering, the biomaterials have an essential role in the presentation of the physiological niche for MSCs allowing encapsulated MSCs viability, and regulating their function and fate.

Studies have confirmed that host pro-inflammatory T-lymphocytes are able to inhibit MSC-mediated bone regeneration through IFN- $\gamma$  (Interferon gamma) induced downregulation of osteogenic regulators (e.g., RUNX2), upregulation of Smad 6, and enhancement of TNF- $\alpha$  (tumor necrosis factor alpha) signaling, which induces cell apoptosis.<sup>[7,8]</sup> However, it is unknown to what extent an implanted biomaterial and its physiochemical properties can serve to regulate the interaction between the MSCs and the host immune system.<sup>[13,14]</sup> It is possible that an encapsulating hydrogel biomaterial, especially in the early stages of implantation, can physically protect implanted MSCs from the host immune cell/cytokine insult and regulate the crosstalk between immune cells and MSCs. Given the increased use of ionically crosslinked hydrogels for stem cell encapsulation,<sup>[15-17]</sup> it is important to

understand the mechanisms that the encapsulating hydrogel uses to regulate the MSC-host immune system interplay and to modulate the fate of the encapsulated stem cells.

Here, we report that alginate hydrogel, as an example of encapsulating biomaterial, affects this interplay when used to encapsulate MSCs for implantation by hindering the penetration of pro-inflammatory cells and/or cytokines, leading to improved viability of the encapsulated MSCs. Our findings suggest that the encapsulating hydrogel depending on its physiochemical properties (e.g., pore size) can affect MSC viability, function and therefore regulate the MSC-host immune cell interplay and direct the fate of the implanted MSCs, leading to enhanced tissue regeneration.

## 2. Results

### 2.1. Host Pro-Inflammatory T-Lymphocytes and Cytokines Inhibit Bone Marrow Mesenchymal Stem Cell (BMMSC)-Mediated Bone Regeneration

To address our research question, we encapsulated human bone marrow (hBM) MSCs in RGD (Arginylglycylaspartic acid)-coupled alginate hydrogel and subcutaneously implanted the resultant microspheres into either C57BL/6/J wild type (WT) or immunocompromised (nude) mice. Unexpectedly, we found new bone formation in alginate-BMMSC implants in WT mice (Figure 1a1,2,b1,b2), an outcome which was not found when BMMSCs were implanted with the gold standard scaffold (hydroxyapatite/tricalcium phosphate (HA/TCP), Zimmer Inc.) (Figure 1 a3,b3) or absorbable collagen sponge (ACS) carrier (Figure S1a8, Supporting Information). To confirm the protective role of alginate hydrogel, we utilized it to encapsulate MSCs from another source, namely stem cells from human exfoliated deciduous teeth (SHED). A similar amount of bone to that observed with alginate-BMMSCs implants was formed by SHED encapsulated in alginate when implanted in WT mice (Figure S1a1–a8, Supporting Information), suggesting that the protective role of alginate is not limited to BMMSCs and might be common to other stem cell types. These data indicated that alginate hydrogel can partially protect MSCs against insult from the host immune system when used as a carrier.

Therefore, we hypothesized that the alginate hydrogel protects the encapsulated MSCs against insult from host pro-inflammatory cells and cytokines. To examine this hypothesis, we intravenously infused immunocompromised mice with  $1 \times 10^6$  pro-inflammatory cells of different types, including Pan T cells,  $CD4^+ IL17^+$  (Th17) cells, and macrophages. We subcutaneously implanted alginate-BMMSC microspheres into the same mice and after 8 weeks, the specimens were harvested. We found that Pan T cells and Th17 cells, but not macrophages, dramatically inhibited bone formation when compared to a control group of immunocompromised mice that did not receive any pro-inflammatory cells (Figure 1 a4–6,b4–b6). These data indicate that pro-inflammatory T-lymphocytes pose a major threat to the success of BMMSC-mediated bone regeneration (Figure 1 c,d). To confirm this finding, we intravenously infused  $1 \times 10^6$   $CD4^+ CD25^+ Foxp3^+$  regulatory T cells (Tregs) into WT mice, to reverse the pro-inflammatory action of the endogenous T-lymphocytes. We found that bone formation was significantly increased compared to a WT control group that received no Tregs (Figure 1 a7,8,b7,8). These data prompted us to examine whether alginate

hydrogel delays the infiltration of the pro-inflammatory T-lymphocytes and/or cytokines into the microspheres.

It is well known that interactions between MSCs and biomaterials strongly influence MSC viability, morphological characteristics, and differentiation in therapeutic applications.<sup>[18,19]</sup> Therefore, understanding these interactions is of the utmost importance to ensure high-quality tissue regeneration. It has been shown that differentiation of encapsulated MSCs within ionically crosslinked alginate hydrogels is dictated by matrix stiffness, regulating the fate of the MSCs regardless of cell morphology.<sup>[15–22]</sup> Our studies (Figure S2a–d, Supporting Information) and others<sup>[18,19]</sup> have confirmed that the modulus of elasticity of the encapsulating biomaterial regulates the stem cell lineage differentiation in 3D cultures. Additionally, changes in the macromolecular diffusion characteristics of hydrogel biomaterials are not responsible for the sensitivity of encapsulated MSCs to the elastic modulus of the encapsulating biomaterial.<sup>[23,24]</sup> Hence, through diffusion rate analysis, we found that changes in the elastic modulus of the alginate hydrogel also affected the permeability of the hydrogel and thus modified its diffusion rate (Figure S2e,f, Supporting Information). Based on these empirical outcomes, it was decided to utilize alginate hydrogel with intermediate stiffness ( $E = 22$  kPa) in order to achieve the lowest diffusion rate and therefore the greatest protection for the encapsulated MSCs to promote osteogenic differentiation. The other important physical properties of the encapsulating biomaterial that has significant role of the viability and fate of the encapsulated cells is the porosity of the biomaterials itself. Our previous studies confirmed that the alginate scaffold possesses a porous structure, with 600 nm average pore size (120 nm to 1  $\mu$ m range), making it a selective barrier for cytokines and/or T-lymphocytes; this stands in contrast to ACS, which possesses an average pore size of 200  $\mu$ m. Therefore, it can be envisioned that alginate hydrogel can act as a physical barrier to slow down the penetration of the pro-inflammatory cytokines into the microspheres.

## 2.2. The Encapsulating Biomaterial Hinders the Infiltration of Pro-Inflammatory Cytokines

To evaluate the ability of alginate hydrogel to physically prevent and delay the infiltration of pro-inflammatory cytokines, the permeability of the alginate hydrogel to two representative cytokines, TNF- $\alpha$  and IL-17, was evaluated in vitro with ACS being used as the control scaffold. Each of the scaffolds was immersed for 3 or 7 days in a 2 mL solution containing 200  $\mu$ g mL<sup>-1</sup> of either IL-17 or TNF- $\alpha$ . The amount of each cytokine that diffused into the tested scaffolds was tracked over time using fluorescent microscopy. Our data (Figure 2 a,b) clearly demonstrated that the initial penetration of cytokines into the microstructure of alginate hydrogel, is hindered, thereby protecting the encapsulated MSCs. We observed that greater amounts of cytokines were able to penetrate the ACS scaffold in comparison to the alginate hydrogel ( $P < 0.01$ ) (Figure 2 c,d). The amount of TNF- $\alpha$  that penetrated each material was slightly lower than that of IL-17 at both time points, perhaps due to its larger molecular weight/size (52 vs 35 kDa, respectively). However, no significant difference in penetration for either cytokine was observed after 14 days of immersion ( $P > 0.05$ ). Taken together, these data confirm that alginate hydrogel can act as a physical barrier hindering the initial penetration of pro-inflammatory cytokines (e.g., TNF- $\alpha$  and IL-17), protecting encapsulated MSCs from cytokines elaborated by the host immune system. Moreover, as a

prove of concept study, another type of nanoporous hydrogel system (poly ethylene glycol dimethacrylate, PEGDMA, Sigma, St Louis, Mo) was used to confirm the protective properties of hydrogel biomaterials is dependent on the porosity of the scaffolds which regulates their permeability against pro-inflammatory cytokines and cells. The utilized PEGDMA hydrogel has a comparable porous structure to alginate hydrogel with pore size ranging from of 500 nm to 1  $\mu\text{m}$ .

To further characterize the permeability of the utilized scaffolds and in order to confirm our obtained data, ELISA analysis was used. Briefly, each of the scaffolds were immersed for 3 or 7 days in a 2 mL solution containing 200  $\mu\text{g mL}^{-1}$  of either IL-17 or TNF- $\alpha$ . After 3 and 7 days the scaffolds were removed, washed ( $\times 3$ ) with distilled water, dissolved, and dried. The concentration of the either of cytokines were analyzed using IL-17 and TNF- $\alpha$  ELISA kits (both from BioLegend, San Diego, CA), respectively. Results (Figure 2 e,f) were in good correlation with the abovementioned fluorescence microscopy data demonstrating that a nanoporous hydrogel (alginate and PEGDMA) can hinder the initial penetration of pro-inflammatory cytokines (TNF- $\alpha$  and IL-17) in comparison to a macro-porous scaffold such as ACS.

### 2.3. Alginate Hydrogel Reduces Apoptosis of Implanted BMMSCs via Reduction of Pro-Inflammatory T-Lymphocyte Penetration

Next, we examined whether alginate is selectively impermeable to host inflammatory cells in vivo. We encapsulated BMMSCs in either alginate hydrogel or ACS and subcutaneously implanted them into WT mice for 3 or 7 days. Using immunofluorescence analysis, we found that the infiltration of CD3<sup>+</sup>, CD4<sup>+</sup>, and CD4<sup>+</sup> IL17<sup>+</sup> T-lymphocytes in ACS was significantly greater after 3 and 7 days of implantation in comparison to the alginate scaffold (Figure 3a–f). Importantly, alginate hydrogel was better at preventing pro-inflammatory T-lymphocyte infiltration than the ACS scaffold (Figure 3 a–d). Given the deleterious effects of pro-inflammatory T-lymphocytes on MSC-mediated bone regeneration, this outcome suggests that the alginate hydrogel biomaterial has favorable properties as a carrier for therapeutic delivery and retention of MSCs.

Since we previously demonstrated that apoptosis of implanted BMMSCs resulted in failed bone regeneration,<sup>[7]</sup> we sought to determine whether pro-inflammatory T-lymphocyte infiltration compromised BMMSC constructs by inducing the MSCs to undergo apoptosis. Histoimmunofluorescence assays showed increased colocalization of CD146<sup>+</sup> BMMSCs with the apoptotic marker Annexin V in ACS scaffolds implanted in WT mice for 3 or 7 days (Figures 3 e and 2f), while the alginate hydrogel significantly reduced the number of apoptotic (CD146<sup>+</sup> AnnexinV<sup>+</sup>) BMMSCs observed (Figures 3e and 2f). Altogether, these data provide evidence that the alginate hydrogel scaffold can protect BMMSCs from apoptosis by inhibiting pro-inflammatory T-lymphocyte infiltration, leading to increased MSC viability. In order to confirm our findings and demonstrate that these finding are not unique only to alginate hydrogels, MSCs were encapsulated in another type of hydrogel biomaterial, PEGDMA, with the same porosity characteristics as alginate hydrogel. Results (Figure 3) clearly demonstrate that the encapsulating hydrogel exhibit protective properties,

which is attributed to hindering the infiltration of pro-inflammatory T-lymphocytes, protecting MSC from apoptosis.

#### 2.4. Pro-Inflammatory Cytokines Induce BMMSC Apoptosis and Reduce their Osteogenic Capacity

To identify whether pro-inflammatory T cells induce BMMSC apoptosis, leading to reduced osteogenic capacity, our experimental strategy was to coculture BMMSCs with Th17 or a Pan T cells for 2 days, followed by flow cytometry analysis to examine the percentage of apoptotic BMMSCs identified as double positive for AnnexinV<sup>+</sup> 7AAD<sup>+</sup>. We found that pro-inflammatory cytokines indeed significantly increased the rate of BMMSC apoptosis (Figure 4a). To confirm the link between cytokine-induced BMMSC apoptosis and reduced osteogenic capacity, we cocultured BMMSCs with IL-17 or a combination of TNF- $\alpha$  and INF- $\gamma$  in vitro under osteogenic conditions. We observed that BMMSCs treated with these cytokines exhibited decreased osteogenic differentiation, as indicated by Alizarin red staining of mineralized nodule formation (Figure 4b). As expected, gene expression analysis revealed downregulated expression of the osteogenic-associated genes alkaline phosphatase (ALP) and runt-related transcription factor 2 (RUNX 2) (Figure 4c).

#### 2.5. Pro-Inflammatory Cytokines Activated CASPASE-Dependent Apoptotic Pathway through Nuclear Factor KappaB (NF- $\kappa$ B) Cascades in BMMSCs

Our obtained data prompted us to assess whether the apoptotic cascade was induced by pro-inflammatory cytokines. Previous studies have shown that pro-inflammatory cytokines from both Th17 and Th1 cells can induce NF- $\kappa$ B pathway activity.<sup>[25–29]</sup> Therefore, we examined whether NF- $\kappa$ B cascades were activated in BMMSCs after treatment with either IL-17 or a combination of TNF- $\alpha$  and INF- $\gamma$ . Western blot analysis showed that the levels of proteins associated with the NF- $\kappa$ B cascade, including p-I $\kappa$ B kinase a (p-IKKa), p-I $\kappa$ B, and p-NF- $\kappa$ B, were significantly elevated in BMMSCs after either treatment (Figure 5a). Furthermore, we examined whether activation of the NF- $\kappa$ B cascade can induce expression of the apoptotic pathway, and found that the expression levels of both cleaved (cysteine-dependent aspartate-directed proteases) CASPASE-3 and CASPASE-8 were significantly increased after treatment with either IL-17 or a combination of TNF- $\alpha$  and INF- $\gamma$  (Figure 5 b). Furthermore, Western blot analysis confirmed that encapsulation of MSCs in alginate hydrogel in vitro significantly reduced the activation of NF- $\kappa$ B cascades in BMMSCs in comparison to BMMSCs seeded within ACS and treated with either IL-17 or a combination of TNF- $\alpha$  and INF- $\gamma$ , which showed decreased expression levels of p-NF- $\kappa$ B (Figure 3c). We next implanted BMMSCs subcutaneously into WT mice for 3 or 7 days with alginate hydrogel, PEGDMA hydrogel or ACS scaffolds, followed by histoimmunofluorescence analyses. We found that levels of the apoptotic pathway proteases CASPASE-3 and CASPASE-8 increased significantly between postimplantation days 3 and 7 in the ACS group with macroporous structure (Figure 5d–g). However, the expression levels of both CASPASE-3 and CASPASE-8 were significantly lower in the alginate and PEGDMA hydrogel groups than in the ACS group ( $P < 0.05$ ), indicating that the encapsulating hydrogel (e.g., alginate or PEGDMA) can protect BMMSCs from this apoptotic cascade (Figure 5d–g).



## 2.6. Indomethacin Treatment Rescued Bone Regeneration Ability of Implanted BMMSCs In Vitro

We further hypothesized that in addition to the inherent protective properties of alginate hydrogel to block cytokine diffusion and host inflammatory cell infiltration, the biomaterial can further be modified with an anti-inflammatory agent to protect the encapsulated MSCs from insults from the host immune system, leading to improved viability and osteogenic differentiation of encapsulated MSCs in vivo. It has been reported that NF- $\kappa$ B pathway activation induces COX-2 pathway upregulation.<sup>[30–32]</sup> To test this hypothesis, we sought to augment the protective effects of alginate hydrogel with the goal of regulating the local microenvironment by delivering an immunosuppressive pharmacological agent with anti-inflammatory function, and evaluate its effects on MSC-mediated bone regeneration (Figure S3a,b, Supporting Information). For the immunosuppressive agent we selected indomethacin, a nonsteroidal anti-inflammatory drug that acts primarily as a COX-2 inhibitor and thus can inhibit the function of pro-inflammatory cytokines.<sup>[33–37]</sup> To confirm the effect of indomethacin when delivered along with MSCs encapsulated in alginate hydrogel, we treated BMMSCs with either Th1 or Th17 pro-inflammatory T-lymphocytes alone or combined with indomethacin. We found that pro-inflammatory T-lymphocytes served to inhibit osteogenesis by the BMMSCs in vitro, as reported in our other experiments discussed here. In contrast, indomethacin treatment rescued osteogenesis in a dose-dependent manner, as indicated by Alizarin red staining of mineralized nodules (Figure 6a,b). Western blot analysis was used to identify the expression of the osteogenic genes ALP and RUNX2 after treatment with pro-inflammatory T-lymphocytes. We found that the addition of indomethacin significantly rescued their expression in a dose-dependent manner (Figure 6c,d).

## 2.7. Indomethacin Treatment Rescued Bone Regeneration Ability of Implanted BMMSCs in WT Mouse Model

Our data prompted us to examine the effects of indomethacin on BMMSC-mediated bone regeneration in vivo. Using two different approaches, namely subcutaneous implantation and a critical-size calvarial defect model in WT mice, we found that implantation of BMMSCs with alginate and indomethacin ( $50 \mu\text{g mL}^{-1}$ ) resulted in improved bone regeneration in the ectopic site, as well as improved bone formation in the calvarial defect area, compared to BMMSCs and alginate without indomethacin or alginate alone (Figure 7a–d). Histological analysis confirmed that the addition of indomethacin significantly improved bone formation when compared to BMMSCs and alginate without indomethacin or alginate alone (Figure 7e–h). Furthermore, the levels of the Prostaglandin E2 were evaluated in the local tissues and peripheral blood using a Prostaglandin E2 ELISA Kit two days after subcutaneous implantation of BMMSC alginate constructs with or without indomethacin in WT mice. The results confirmed that the anti-inflammatory drug, indomethacin, exerts its effects in the local tissue without having any systemic effects (Figure 7 i,j). Moreover, the effects of indomethacin drug on local immune response were further evaluated using multicolor flow cytometry analysis. Our data demonstrate (Figure 7k) that, during subcutaneous implantation of encapsulated BMMSCs in alginate hydrogel in WT mice, in presence of indomethacin there was a significant decrease ( $P < 0.05$ ) in the

number of Th1 and Th17 cells in comparison to specimens without indomethacin. These in vivo data corroborated the results of our mechanistic studies, in which we found that protection of implanted BMMSCs from insult by host pro-inflammatory cytokines and cells leads to significant improvement in bone tissue regeneration. To test the potential translational value of these findings, we used indomethacin treatment to inhibit functions of pro-inflammatory cytokines (Figure S3c,3g, Supporting Information), and found a significant improvement in the bone regeneration capacity of BMMSCs (Figure S3e,f, Supporting Information).

### 3. Discussion

MSCs hold great promise to change the face of regenerative medicine. However, an important limitation to clinical application of MSCs is immunological rejection by host immune cells and pro-inflammatory cytokines. Previous work has demonstrated that stem cell-mediated bone regeneration is partially controlled by the local microenvironment, including the presence of growth factors, recipient immune cells and cytokines.<sup>[7]</sup> In particular, pro-inflammatory T cells are able to inhibit MSC-mediated bone regeneration through IFN- $\gamma$ -induced downregulation of osteogenesis regulators and enhancement of TNF- $\alpha$  signaling in induced cell apoptosis.<sup>[7]</sup> In the current study, we demonstrate that pro-inflammatory T cells and not macrophages MSC-mediated bone regeneration. Macrophages play an important role in regulation of the inflammatory responses and tissue regeneration. Recently, it has been reported that hydrogel delivery systems containing macrophage recruitment agents, are capable of enhance the bone regeneration in animal models.<sup>[51]</sup>

It is well known that the anti-inflammatory effect of indomethacin is through inhibition of COX-2 activity and therefore inhibition of prostaglandin synthesis.<sup>[38,39]</sup> Studies have shown that PGE<sub>2</sub> can regulate multiple aspects of inflammation and multiple functions of different immune cells.<sup>[40]</sup> It has been generally recognized as a mediator of active inflammation, promoting local vasodilatation and local attraction and activation of neutrophils, macrophages, and mast cells at early stages of inflammation.<sup>[41]</sup> In addition, it has been reported that PGE<sub>2</sub> can promote the development of IL-17-producing T cells, which is related to PGE<sub>2</sub> ability to suppress the production of IL-12p70 (Th17-inhibitory) while enhancing the Th17-supporting IL-23.<sup>[42,43]</sup> Other studies have confirmed that induction of COX-2 expression lead to the production of prostaglandins (PGE<sub>2</sub>) that will enhance IL-17 synthesis leading to inflammation and tissue breakdown.<sup>[44]</sup> In the current study, we demonstrate that administration of indomethacin, locally not systemically, significantly reduced the number of the Th1 and Th17 cells in the local microenvironment that well correlated to the viability and osteogenic differentiation of implanted MSCs. Another beneficial effect of the anti-inflammatory drugs (e.g., indomethacin), which is more important in the later stages of transplantation, is their inhibitory effects on formation of fibrotic cell layers and collagen deposition on the surface of transplanted microspheres, hence, enhancing the viability and function of the encapsulated MSCs in a broad range of cell-based therapeutics.<sup>[45,46]</sup> Therefore, local administration of anti-inflammatory drugs via hydrogel delivery vehicles can be used as a strategy to mitigate host immune response and improve the stability of implantable biomedical devices.<sup>[47]</sup>

In studying the role of biomaterials in the MSC-host immune system interplay, hydrogel biomaterials (e.g., alginate) carry specific advantages. Hydrogel materials allow control over the amount and spatial presentation of MSCs during and after delivery, enabling us to perform systematic examination of the effects of the alginate hydrogel on this interplay.<sup>[48–50]</sup> In comparison to other biomaterials, such as HA/TCP or ACS, hydrogel biomaterials can encapsulate MSCs, and may thus act as a physical barrier between the cells and the host immune system. Here we demonstrated that by encapsulating MSCs in an RGD-coupled alginate 3D scaffold, we can provide an appropriate physiochemical microenvironment for enhanced MSC adhesion and viability, and in addition, we are able to protect the MSCs from the host immune system via physical separation in the early stages of transplantation. This protective property is exerted through hindering the infiltration of pro-inflammatory cytokines and cells. Moreover, the presence of the encapsulating biomaterial prevents and delays the direct cell-to-cell contact, which enhances cell viability and function.<sup>[44]</sup>

Additionally, it has been shown that the mechanical properties of the encapsulating hydrogel including modulus influence stem cell viability and fate.<sup>[11–15]</sup> We observed the same phenomenon in the current study and based on our empirical data, it was decided to utilize alginate hydrogel with intermediate stiffness ( $E = 22$  kPa) in order to achieve the lowest diffusion rate and therefore the greatest protection for the encapsulated MSCs to promote osteogenic differentiation. Furthermore, we confirmed that scaffold morphology, in terms of pore-size is another crucial parameter to be considered in the stem cell-immune cell interplay. Alginate or PEGDMA hydrogel with nanoporous structure can hinder the penetration of pro-inflammatory cytokines and cells while providing adequate transport of nutrients and oxygen leading to improved cell viability and osteogenesis. Our results confirmed the possibility of extending and improving MSC viability and, therefore, correspondingly improving the tissue regeneration capacity of MSCs by encapsulating them in a 3D scaffold, which protects them from host immune cells and cytokines. In addition, by incorporating indomethacin in our MSC delivery system, tested in a WT animal model, we further regulated the host local microenvironment, leading to additional improvements in the tissue regeneration capacity of the encapsulated MSCs.

## 4. Conclusions

Taken together, these findings substantially extend current knowledge concerning the role of biomaterials in MSC-mediated tissue regeneration and provide a new strategy for enhanced bone regeneration in MSC-mediated therapies. We also demonstrate that an alginate hydrogel scaffold protects MSCs by regulating the interplay between the MSCs and the host immune system in MSC-mediated bone tissue engineering, thereby providing a molecular and cellular basis for improving the application of hydrogels in stem cell-based therapies.

## 5. Experimental Section

### Animals

All the animal experiments were performed in accordance with Institutional Animal Care and Use Committee (IACUC)-approved small animal protocols (11327 and 11953) at the

University of Southern California. Female C57BL6J and immunocompromised nude (Beige nu/nu XIDIII) mice were purchased from Jackson Laboratories and Harlan Laboratories, respectively. In each of the animal experiments five mice ( $N = 5$ ) were used for each group.

### Progenitor Cell Isolation, Culture and Encapsulation

Human BMMSCs, processed from marrow aspirates of normal human adult volunteers (20–35 years of age), were utilized. SHED were harvested and cultured according to published protocols with Institutional Review Board (IRB) approval from the University of Southern California (HS 07-00701).<sup>[52]</sup> The cells were cultured for two weeks with alpha minimum essential medium (MEM) (Invitrogen) supplemented with 50% fetal bovine serum (FBS),  $2 \times 10^{-3}$  M l-glutamine (Invitrogen),  $100 \times 10^{-6}$  M ascorbic acid-2-phosphate (Wako Chemicals USA),  $100 \text{ U mL}^{-1}$  penicillin, and  $100 \text{ g mL}^{-1}$  streptomycin (Invitrogen). Flow cytometric analysis was performed to ensure that the BMMSCs and SHED were positive for MSC surface markers CD73, CD146, CD166, and Sca-1 and negative for hematopoietic cell markers CD31, CD34, and CD45 (BD Biosciences, San Jose, CA). Passage four cells were used in all the experiments.

### Biomaterials Fabrication and Cell Encapsulation

Custom-made RGD-coupled alginate ( $M_w$ : 150 kDa, G/M  $\geq 1.5$ , Nova Matrix, Norway) was utilized after charcoal treatment and oxidization (2%) using Sodium Periodate (Sigma, St. Louis, MO), to increase its degradability by production of hydrolytically labile bonds, according to previously published methods.<sup>[53,54]</sup> Next, the alginate solution was filtered through sterile  $0.22 \mu\text{m}$  filters (Millipore, Billerica, MA). BMMSCs or SHED were encapsulated in the RGD-coupled alginate at different cell densities. The alginate hydrogel microspheres formation was accomplished by extruding alginate-MSD droplets through a syringe into a solution of  $100 \times 10^{-3}$  M calcium chloride ( $\text{CaCl}_2$ ). The alginate droplets cross-linked and formed microspheres. The constructs were formed microspheres at  $37^\circ\text{C}$  for 45 min to form completely cross-linked spheres and then washed three times in nonsupplemented Dulbecco's Modified Eagle's medium (DMEM). No appearance of stem cells in each well, confirmed the encapsulation of the stem cells to the hydrogel spherical construct. Alginate microspheres without cells were used as negative controls. ACS (Helicote, Plainsboro, NJ), a nonencapsulating carrier biomaterial, was used as a control MSC delivery vehicle. Commercially available poly (ethylene glycol) dimethacrylate (PEGDMA with average  $M_n$ : 550, Sigma) was sterilized under UV light overnight, dissolved in 10 mL PBS and  $100 \mu\text{L}$  Pen/strep.  $200 \mu\text{L}$  of 5% photoinitiator (2-Hydroxy-4'-(2-hydroxyethoxy)-2-methylpropiophenone, Sigma) solution in 100% ethanol was added to PEGDMA solution and MSC were mixed with PEG at  $2 \times 10^6$  cells  $\text{mL}^{-1}$ . A total of  $500 \mu\text{L}$  of cell/PEG solution was loaded and polymerized for 10 min using 365 nm long wavelength UV light.

### Biomaterial Mechanical Properties Characterization and Effects on Permeability and Encapsulated MSC Differentiation

The compressive moduli of alginate hydrogels with different calcium ion concentrations were determined according to methods already in the literature.<sup>[21]</sup> The Young's modulus of

the hydrogel was then determined using the slope of the stress–strain curve at low strain. Additionally, the release profiles of bovine serum albumin (BSA, 67 kDa, Sigma) incorporated into alginate microspheres with different degrees of elasticity were determined. To measure the BSA diffusion out of alginate hydrogel, alginate microspheres were immersed in PBS solution and the amount of released protein was analyzed with a UV spectrophotometer at 320 nm (Beckman, Brea, CA) at time points up to two weeks. Additionally, BMMSCs were encapsulated in RGD-coupled alginate hydrogels with different elastic modulus (5–50 KPa) and utilized in an in vitro osteogenic analysis. After 4 weeks of osteogenesis, the degree of the osteo-differentiation was analyzed using xylenol orange (XO, a fluorescent probe which distinguishes the presence of calcified deposits) and analysis of ALP levels using a colorimetric p-nitro-phenyl phosphate assay according to manufacturer's instructions (Abcam, Cambridge, MA).

### Permeability Analysis of Alginate Hydrogels In Vitro

The permeability of the alginate hydrogel and PEGDMA to two representative cytokines, TNF- $\alpha$  and IL-17, was evaluated in vitro with ACS being used as the control scaffold. Scaffolds were immersed for 3 or 7 days in a 2 mL solution containing 200  $\mu\text{g mL}^{-1}$  of either IL-17 or TNF- $\alpha$ . The amount of each cytokine that diffused into the tested scaffolds was tracked over time using fluorescent microscopy utilizing antibodies against IL-17 and TNF- $\alpha$  (Abcam). Additionally, the concentrations of cytokines (TNF- $\alpha$ , IL17) infiltrated into each scaffold were measured using IL-17 and TNF- $\alpha$  ELISA (enzyme-linked immunosorbent assay) kits (both from BioLegend, San Diego, CA) after 3 and 7 days.

### Evaluation of the Shielding Properties of Encapsulating Scaffold In Vivo

Encapsulated BMMSCs ( $2 \times 10^6$ ) were transplanted subcutaneously into the dorsal surface of WT mice (C57BL/6). The specimens were harvested after 3 or 7 days and the degree of the penetration of pro-inflammatory T-lymphocytes was analyzed immunofluorescently using CD3, CD4, IL-17, and CD146 (MSC marker) antibodies (counterstained with DAPI) using confocal laser scanning microscopy (CLSM). BMMSCs seeded within ACS or encapsulated in PEGDMA hydrogel were used as controls.

### Cell Apoptosis Evaluation

BMMSCs ( $0.5 \times 10^6$ ) were seeded on six-well culture plates and cocultured with Pan-T or Th-17 cells for 3 days. BMMSC apoptosis was analyzed using FACSCalibur (BD Bioscience) flow cytometric evaluation by staining the cells with Annexin V-PE Apoptosis Detection Kit I (BD Bioscience).

### In Vitro Osteogenic Differentiation of MSCs in the Presence of pro-inflammatory Cytokines

BMMSCs were cultured in osteogenic medium for 4 weeks. Three types of cytokines: IL-17 ( $20 \text{ ng mL}^{-1}$ ), IFN- $\gamma$  ( $50 \text{ ng mL}^{-1}$ ), TNF- $\alpha$  ( $20 \text{ ng mL}^{-1}$ ) (BioLegend, San Diego CA) were added to the osteogenic culture medium every 3 days. After 4 weeks of osteogenic induction, the cultures were stained with Alizarin red. The expression levels of Runx2 and ALP (Santa Cruz Biosciences, Dallas, TX) were assayed by Western blot.

## Effects of Immune Cells on Bone Regenerative Properties of Encapsulated MSCs In Vivo

Pan T cells, CD4<sup>+</sup> CD25<sup>-</sup> T-lymphocytes, CD4<sup>+</sup> CD25<sup>+</sup> Foxp<sup>3+</sup> Treg lymphocytes, and macrophages were isolated according to previously published methods.<sup>7</sup> Subsequently, encapsulated BMSCs or SHED ( $2 \times 10^6$  cells mL<sup>-1</sup> alginate) were subcutaneously transplanted into immunocompromised mice. Approximately  $1 \times 10^6$  of each of the isolated immune cells (PanT, Th17, and macrophage) were suspended in 200  $\mu$ L PBS and injected into the mice via the tail vein immediately prior to the surgical procedure. Additionally, encapsulated BMSCs or SHED ( $2 \times 10^6$  cells mL<sup>-1</sup> alginate) were subcutaneously transplanted into C57BL/6 mice and  $\approx 1 \times 10^6$  Tregs were suspended in 200  $\mu$ L PBS and injected into the mice via the tail vein immediately prior to the surgical procedure. Eight weeks after transplantation, the implants were harvested and the amount of bone regeneration was quantified using radiographic examination, micro-CT, and histological analyses. For comparison, ACS and HA/TCP scaffolds were used as the control. When the implants were harvested at 1, 5, 7, or 14 days, the concentrations of cytokines (IFN- $\gamma$ , TNF- $\alpha$ , IL17) were measured using mouse IFN- $\gamma$ , TNF- $\alpha$  (eBioscience, San Diego, CA), and IL-17 ELISA kits (Invitrogen).

## Development of MSC-Based Drug Delivery System

RGD-coupled alginate as mentioned above was dissolved in deionized water (1% w/v) and prepared as mentioned before. Next, alginate was mixed with indomethacin (Sigma) at 0.25%, 0.5%, or 1% (w/v) under rigorous stirring overnight. MSCs were encapsulated in alginate according to the methods mentioned earlier.

## In Vitro Drug Release

Ten alginate microspheres (containing 0.25%, 0.5%, or 1% (w/v) of indomethacin) with predetermined weight and volume were suspended in 5 mL of PBS (pH = 7.4). The solution was stirred at 50 rpm using a magnetic stirrer and maintained at 37 °C. At several time points (0–100 h), 2 mL of the sample was removed and the amount of released indomethacin was analyzed with a UV spectrophotometer at 320 nm (Beckman, Brea, CA). The same volume of fresh medium was introduced to replace the withdrawn sample.

## Analysis of Effects of Indomethacin Administration on MSC Survival In Vitro

BMSCs ( $1 \times 10^6$ ) encapsulated in alginate hydrogel with indomethacin ( $50 \mu$ g mL<sup>-1</sup>) were cultured in the presence of select inflammatory cytokines IL-10 (20 ng mL<sup>-1</sup>), or IL-17 (20 ng mL<sup>-1</sup>), or TNF- $\alpha$  (20 ng mL<sup>-1</sup>) combined with IFN- $\gamma$  ( $50 \text{ ng mL}^{-1}$ ) for 2 days. After 48 h of culturing, the apoptotic MSCs were detected by staining with antibodies against Annexin V-PE (BD Pharmingen). The control group did not have any indomethacin added. Also, encapsulated BMSCs containing indomethacin ( $50 \mu$ g mL<sup>-1</sup>) were cultured in osteogenic media in the presence of select inflammatory cytokines IL-10 (20 ng mL<sup>-1</sup>), or IL-17 (20 ng mL<sup>-1</sup>), TNF- $\alpha$  (20 ng mL<sup>-1</sup>) combined with IFN- $\gamma$  ( $50 \text{ ng mL}^{-1}$ ) for two weeks. The ALP concentrations were measured using a colorimetric p-nitro-phenyl phosphate assay (Abcam).

### **In Vitro Osteogenic Differentiation Assay: Effects of Administration of Indomethacin**

BMMSCs ( $0.2 \times 10^6$ ) were cocultured under osteogenic culture conditions in the presence of Th17 cells ( $1 \times 10^6$ ). To study the effect of the anti-inflammatory drug on osteogenesis, indomethacin (at a dose of 10 or  $50 \mu\text{g mL}^{-1}$ ) was added to the osteogenic differentiation media every 3 days. After 4 weeks of treatment the samples were stained with Alizarin red. Also, the expression levels of Runx2 and ALP were assayed by Western blot according to the methods mentioned earlier. The same experiment was conducted in the presence of CD3 activated T cells. In order to study the protective properties of the encapsulating hydrogel, encapsulated BMMSCs containing indomethacin (at a dose of 10 or  $50 \mu\text{g mL}^{-1}$ ) were cultured in osteogenic media in the presence of Th17 cells, and after 4 weeks of culturing, the samples were stained with antibodies against ALP. In addition, after dissolving the alginate microspheres in citrate buffer (6% w/v, PH = 7.4) and extracting the protein, the expression levels of Runx2 and ALP were examined by Western blot. MSCs without indomethacin and samples without Th17 cells were used as the control groups.

### **BMMSC-Mediated Bone Formation: Effects of Administration of Indomethacin**

Approximately  $2.0 \times 10^6$  BMMSCs were encapsulated in alginate hydrogel containing indomethacin and subcutaneously implanted into the dorsal surface of C57BL/6J mice. Eight weeks after implantation, the implants were harvested. Micro-CT analysis and H&E staining of the histological sections were evaluated using the NIH ImageJ software. MSC hydrogel constructs were implanted subcutaneously in immunocompromised mice as positive control, while the constructs without indomethacin or without BMMSCs were used in WT mice as the negative controls.

### **Calvarial Bone Defect Model in C57BL/6J Mice: Effects of Administration of Indomethacin**

Approximately  $4 \times 10^6$  BMMSCs were encapsulated in alginate hydrogel containing indomethacin and implanted into 5 mm diameter defects in the calvaria of C57BL/6J mice according to previously published methods.<sup>7</sup> MSCs encapsulated in alginate without indomethacin and alginate hydrogel alone were used as controls. To study the role of the anti-inflammatory agent in vivo, the cytokine levels in the implants were measured. Briefly,  $4 \times 10^6$  BMMSCs were encapsulated in alginate hydrogel containing indomethacin and transplanted into 5 mm diameter defects in the calvaria of C57BL/6J mice.

### **Cytokine Levels in BMMSC-Mediated Bone Formation: Effects of Administration of Indomethacin**

The implants were harvested at different time points (1, 3, 7, and 14 days) and the levels of cytokines (IFN- $\gamma$ , TNF- $\alpha$ , IL17) were measured using mouse IFN- $\gamma$ , TNF- $\alpha$  (eBioscience, San Diego, CA), and IL-17 ELISA kits (Invitrogen).

### **Measurement of Local and Systemic PGE2 Levels**

BMMSCs ( $2.0 \times 10^6$ ) were encapsulated in alginate hydrogel containing indomethacin and subcutaneously implanted into the dorsal surface of C57BL/6J mice. Two days after implantation, the specimens were retrieved for local measurements of PGE2 levels. The retrieved specimens with the attached tissue were prepared, centrifuged, and the supernatant

solutions were used for the prostaglandin E2 assay. The prostaglandin E2 concentration was then assayed using Prostaglandin E2 ELISA Kit (Abcam). Additionally, The plasma levels of PGE2 were measured using ELISA assay following manufacturer's instructions (Abcam).

### Multicolor Flow Cytometry

Approximately  $2.0 \times 10^6$  BMMSCs were encapsulated in alginate hydrogel containing indomethacin and subcutaneously implanted into the dorsal surface of C57BL/6J mice. Two days after implantation, the specimens were retrieved. Present Th1 and Th17 cells were identified and quantified using FITC (fluorescein isothiocyanate)- and PE-labeled antibodies against CD3, INF- $\gamma$ , and IL-17.

### Statistical Analysis of Data

As appropriate, data were analyzed statistically by means of a Student's *t* test, Mann–Whitney *U* test, analysis of variance (ANOVA), or Kruskal–Wallis test.  $P < 0.05$  was considered significant. SPSS 16.0 was used for statistical analysis of data.

### Supplementary Material

Refer to Web version on PubMed Central for supplementary material.

### Acknowledgments

A.M. and C.C. contributed equally to this work. This work was supported by grants from the National Institute of Dental and Craniofacial Research, National Institutes of Health, Department of Health and Human Services (K08DE023825 to A.M., R01DE017449 and R01 DE019932 to S.S.); and a grant from the California Institute for Regenerative Medicine (RN1-00572 for S.S.).

### References

1. Chen FM, Zhang J, Zhang M, An Y, Chen F, Wu ZF. *Biomaterials*. 2010; 31:7892. [PubMed: 20684986]
2. Sachlos E, Czernuszka JT. *Eur Cells Mater*. 2003; 5:29.
3. Monaco E, Bionaz M, Hollister SJ, Wheeler MB. *Theriogenology*. 2011; 75:1381. [PubMed: 21354606]
4. Caplan AI. *J Cell Physiol*. 2007; 213:341. [PubMed: 17620285]
5. García-Gómez I, Elvira G, Zapata AG, Lamana ML, Ramírez M, Castro JG, Arranz MG, Vicente A, Bueren J, García-Olmo D. *Expert Opin Biol Ther*. 2010; 10:1453. [PubMed: 20831449]
6. Tasso R, Fais F, Reverberi D, Tortelli F, Cancedda R. *Biomaterials*. 2010; 31:2121. [PubMed: 20004968]
7. Liu Y, Wang L, Kikuri T, Akiyama K, Chen C, Xu X, Yang R, Chen W, Wang S, Shi S. *Nat Med*. 2011; 17:1594. [PubMed: 22101767]
8. Liu Y, Wang S, Shi S. *Int J Biochem Cell Biol*. 2012; 44:2044. [PubMed: 22903019]
9. Moshaverinia A, Ansari S, Chen C, Xu X, Akiyama K, Snead ML, Zadeh H, Shi S. *Biomaterials*. 2013; 34:6572. [PubMed: 23773817]
10. Ansari S, Moshaverinia A, Han A, Pi SH, Abdelhamid AI, Zadeh HH. *Biomaterials*. 2013; 34:10191. [PubMed: 24055525]
11. Anderson SB, Lin CC, Kuntzler DV, Anseth KS. *Biomaterials*. 2011; 32:3564. [PubMed: 21334063]
12. BiaN L, Guvendiren M, Mauck RL, Burdick JA. *Proc Natl Acad Sci USA*. 2013; 110:10117. [PubMed: 23733927]



13. Huebsch N, Mooney DJ. *Nature*. 2009; 462:426. [PubMed: 19940912]
14. Nilsson B, Korsgren O, Lambris JD, Ekdahl KN. *Trends Immunol*. 2010; 31:32. [PubMed: 19836998]
15. Khetan S, Guvendiren M, Legant WR, Cohen DM, Chen CS, Burdick JA. *Nat Mater*. 2013; 12:458. [PubMed: 23524375]
16. Benoit DS, Schwartz MP, Durney AR, Anseth KS. *Nat Mater*. 2008; 7:816. [PubMed: 18724374]
17. Huebsch N, Arany PR, Mao AS, Shvartsman D, Ali OA, Bencheri SA, Rivera-Feliciano J, Mooney DJ. *Nat Mater*. 2010; 9:518. [PubMed: 20418863]
18. Docheva D, Popov C, Mutschler W, Schiekier M. *J Cell Mol Med*. 2007; 11:21. [PubMed: 17367499]
19. Meredith JE Jr, Fazeli B, Schwartz MA. *Mol Biol Cell*. 1993; 4:953. [PubMed: 8257797]
20. Ruoslahti E, Reed JC. *Cell*. 1994; 77:477. [PubMed: 8187171]
21. VandeVondele S, Vörös JA, Hubbell JA. *Biotechnol Bioeng*. 2003; 82:784. [PubMed: 12701144]
22. Gillette BM, Jensen JA, Tang B, Yang GJ, Bazargan-Lari A, Zhong M, Sia SK. *Nat Mater*. 2008; 7:636. [PubMed: 18511938]
23. Ghajar CM, Chen X, Harris JW, Suresh V, Hughes CC, Jeon NL, Putnam AJ, George SC. *Biophys J*. 2008; 94:1930. [PubMed: 17993494]
24. Boonthekul T, Kong HJ, Mooney DJ. *Biomaterials*. 2005; 26:2455. [PubMed: 15585248]
25. Maitra A, Shen F, Hanel W, Mossman K, Tocker J, Swart D, Gaffen SL. *Proc Natl Acad Sci USA*. 2007; 104:7506. [PubMed: 17456598]
26. Qian Y, Liu C, Hartupee J, Altuntas CZ, Gulen MF, Jane-Wit D, Xiao J, Lu Y, Giltiay N, Liu J, Kordula T, Zhang QW, Vallance B, Swaidani S, Aronica M, Tuohy VK, Hamilton T, Li X. *Nat Immunol*. 2008; 8:247. [PubMed: 17277779]
27. Xie S, Li J, Wang JH, Wu Q, Yang P, Hsu HC, Smythies LE, Mountz JD. *J Immunol*. 2010; 184:2289. [PubMed: 20139273]
28. Fichtner-Feigl S, Fuss IJ, Preiss JC, Trober W, Kitani A. *J Clin Invest*. 2005; 15:3057. [PubMed: 16239967]
29. Chang J, Liu F, Lee M, Wu B, Ting K, Zara JN, Soo C, Al Hezaimi K, Zoug W, Chen X, Mooney DJ, Wang CY. *Proc Natl Acad Sci USA*. 2013; 110:9469. [PubMed: 23690607]
30. Jung YJ, Isaacs JS, Lee S, Trepel J, Neckers L. *FASEB J*. 2003; 17:2115. [PubMed: 12958148]
31. Nakao S, Ogtata Y, Shimizu E, Yamazaki M, Furuyama S, Sugiyama H. *Mol Cell Biochem*. 2002; 238:11. [PubMed: 12349897]
32. Lin CC, Hsieh HL, Shih RH, Chi PL, Cheng SE, Yang CM. *Cell Commun Signaling*. 2013; 11:8.
33. Nalbant S, Akmaz I, Kaplan M, Avsar K, Solmazgul E, Sahar B. *Clin Exp Rheumatol*. 2006; 24:361. [PubMed: 16956424]
34. Taki H, Sugiyama E, Mino T, Kuroda A, Kobayashi M. *Clin Exp Immunol*. 1998; 11:133. [PubMed: 9566801]
35. Sirota L, Punskey I, Bessler H. *Acta Paediatr*. 2000; 89:331. [PubMed: 10772282]
36. Shi J, Alves NM, Mano JF. *J Biomed Mater Res Part B*. 2008; 84:595.
37. Xin J, Guo Z, Chen X, Jiang W, Li J, Li M. *Int J Pharm*. 2010; 386:221. [PubMed: 19945520]
38. Simon LS. *Am J Med*. 1999; 106:37.
39. Suleyman HZ, Halici E, Cadirci A, Hacimuftuoglu A, Bilen H. *J Physiol Pharm*. 2008; 59:661.
40. Phipps RP, Stein SH, Roper RL. *Immunol Today*. 1991; 12:349. [PubMed: 1958288]
41. Durand EM, Zon LI. *Curr Opin Hematol*. 2010; 17:308. [PubMed: 20473159]
42. Boniface K, Bak-Jensen KS, Li Y, Blumenschein WM, McGeachy MJ, McClanahan TK, McKenzie BS, Kastelein RA, Cua DJ, de Waal Malefyt R. *J Exp Med*. 2009; 206:535. [PubMed: 19273625]
43. Khayrullina T, Yen JH, Jing H, Ganea D. *J Immunol*. 2008; 181:721. [PubMed: 18566439]
44. Lemos HP, Grespan R, Vieira SM, Cunha TM Jr, Verri WA, Fernandes KS. *Proc Natl Acad Sci USA*. 2009; 106:5954. [PubMed: 19289819]
45. Van Schilfgaarde R, DeVos P. *J Mol Med*. 1999; 77:199. [PubMed: 9930963]

46. Bunker CM, Tiefenbach B, Jahnke A, Gerlach C, Freier T, Schmitz KP. *Biomaterials*. 2005; 26:2353. [PubMed: 15585238]
47. Dang TT, Thai AV, Cohen J, Slosberg JE, Siniakowicz K, Doloff JC. *Biomaterials*. 2013; 34:5792. [PubMed: 23660251]
48. Hatch A, Hansmann G, Murthy SK. *Langmuir*. 2011; 27:4257. [PubMed: 21401041]
49. Higasi T, Nagamori E, Sone T, Matsunaga S, Fukui KA. *J Biosci Bioeng*. 2004; 97:191. [PubMed: 16233613]
50. Augst AD, Kong HJ, Mooney DJ. *Macromol Biosci*. 2006; 6:623. [PubMed: 16881042]
51. Kim HK, Furuya H, Tabata Y. *Biomaterials*. 2014; 35:214. [PubMed: 24125774]
52. Seo BM, Sonoyama W, Yamaza T, Coppe C, Kikuri T, Akiyama K, Lee JS, Shi S. *Oral Dis*. 2008; 14:428. [PubMed: 18938268]
53. Moshaverinia A, Chen C, Akiyama K, Xu X, Ansari S, Zadeh HH, Shi S. *Tissue Eng Part A*. 2014; 20:611. [PubMed: 24070211]
54. Moshaverinia A, Chen C, Akiyama K, Xu X, Chee WW, Schricker SR, Shi S. *J Biomed Mater Res Part A*. 2013; 101:3285.

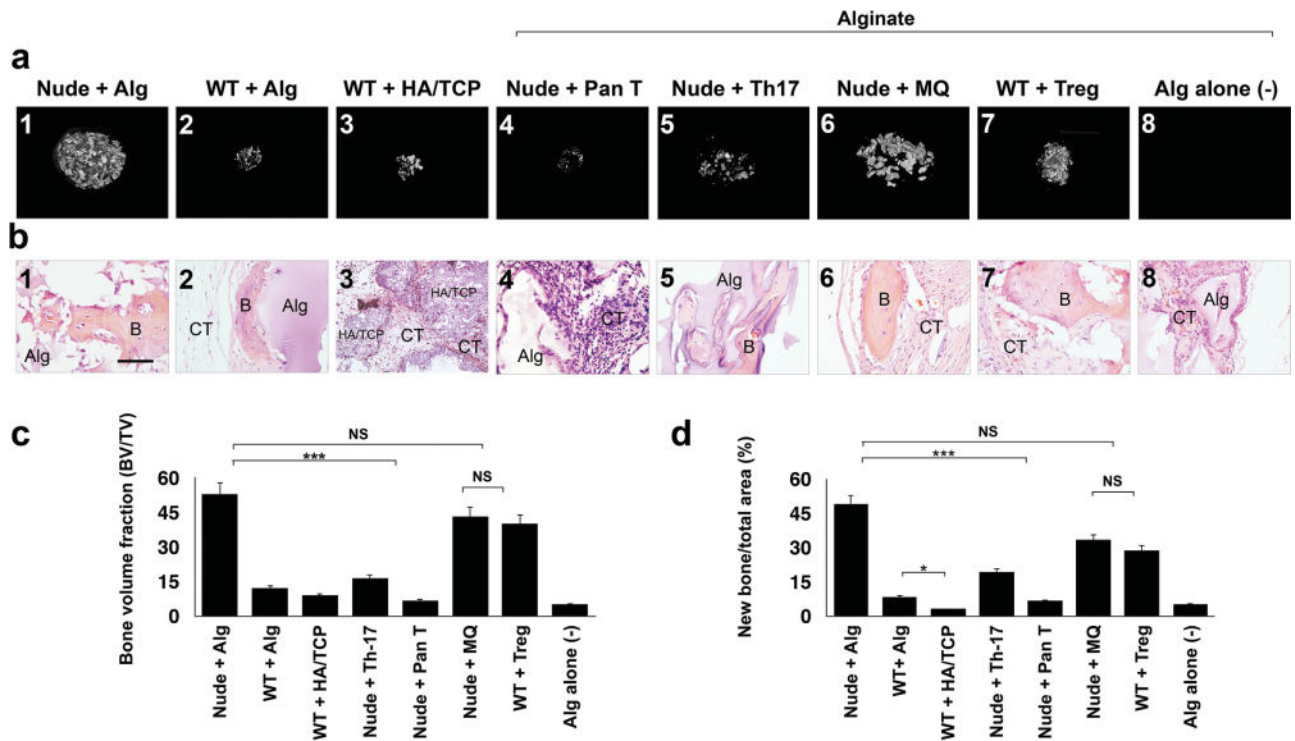


**Figure 1.** Host pro-inflammatory T-lymphocytes and cytokines inhibit BMMSC-mediated bone regeneration. a) Microtomography or corresponding histological b) analyses of bone regeneration after  $\approx 2 \times 10^6$  BMMSCs encapsulated into 1 mL of RGD-coupled alginate and were subcutaneously implanted into immunocompromised mice (a1,b1), C57BL/6 WT mice (a2,b2), or transplanted with HA/TCP into C57BL/6 WT mice (a3,b3), and analyzed after 8 weeks. The role of pro-inflammatory cells on bone formation was tested by supplementing immunocompromised mice with  $\approx 1 \times 10^6$  each of previously isolated PanT a4,b4), Th17 a5,b5), or macrophage (MQ) a6,b6) immune cells, with each cell type suspended in 200  $\mu$ L PBS and injected into the host mice via the tail vein immediately prior to surgically implanting the BMMSC-alginate construct. Bone formation by the alginate-encapsulated BMMSCs could be partially rescued by supplementing the C57BL/6 WT host with  $1 \times 10^6$  isolated Treg cells suspended in 200  $\mu$ L PBS injected via the tail vein immediately prior to surgically implanting the BMMSC-alginate construct. Subcutaneous engraftment of BMMSCs encapsulated in alginate hydrogel in immunocompromised mice showed the greatest amount of bone formation compared to WT hosts, with increased bone production in WT hosts supplemented with Treg cells. pro-inflammatory T cells, but not macrophages, diminished bone production. RGD-coupled alginate alone showed no bone regeneration (a8,b8). c) Shown in (a1–a8) are samples subjected to bone volume (BV) fraction measurement derived from BV/total volume (TV) as assessed by micro-CT or d) bone volume/total area identified by histomorphometric analysis. Scale bars: b), 200  $\mu$ m; Alg = alginate; B = Bone; CT = connective tissue. Each error bar represents the standard deviation; NS = not significant; \*  $P < 0.05$  and \*\*\*  $P < 0.001$ . Kruskal–Wallis test was utilized to compare and analyze the obtained data.

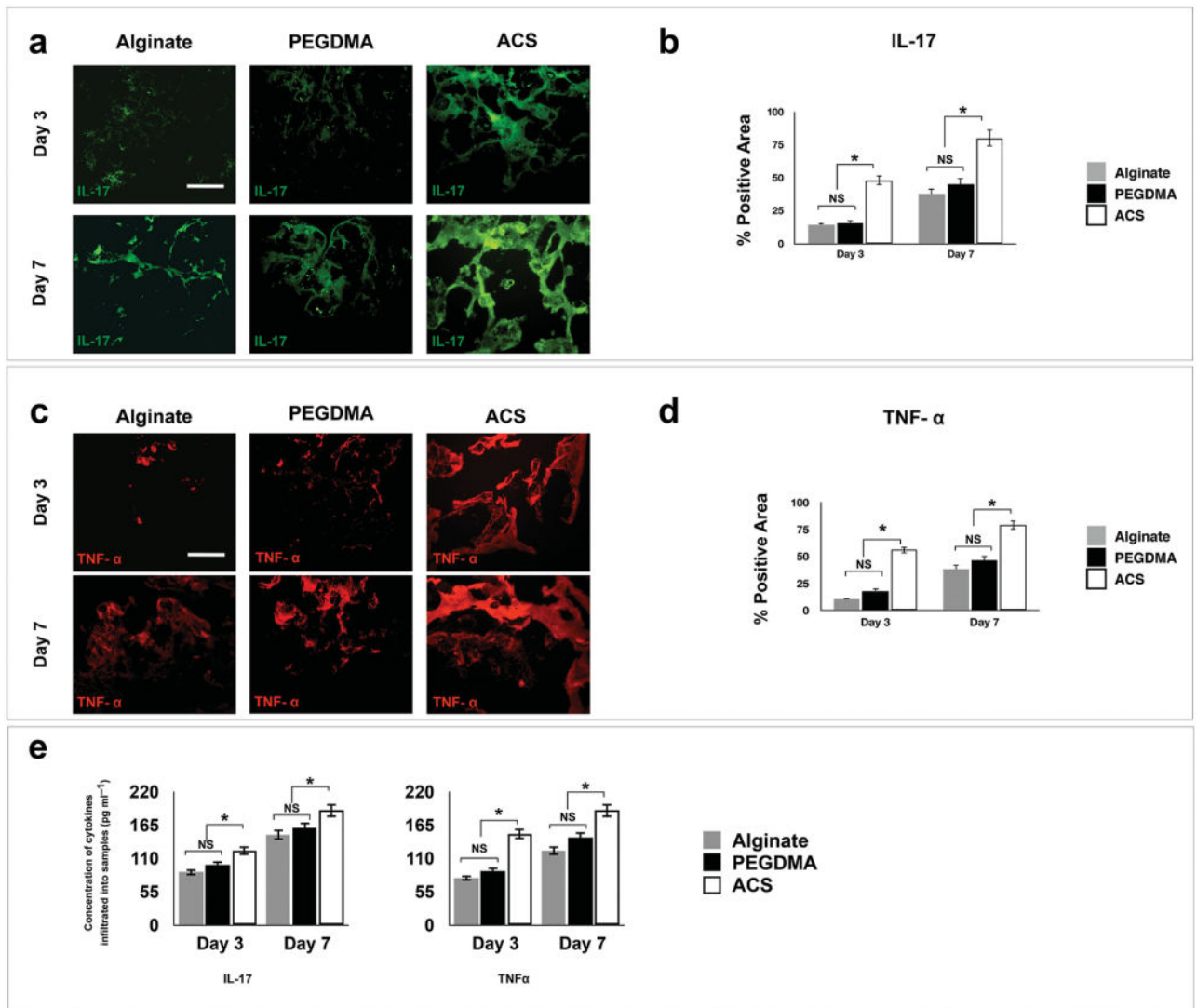


**Figure 2.**

The encapsulating biomaterial hinders the infiltration of pro-inflammatory cytokines. Characterization of the permeability of fabricated alginate microspheres or PEGDMA hydrogel to a,b) IL-17 or c,d) TNF- $\alpha$  using immunofluorescence techniques. Immunofluorescence staining showed infiltration of pro-inflammatory cytokines IL-17 (a) or TNF- $\alpha$  (c) is reduced in alginate or PEGDMA (c) compared to d) ACS after 3 or 7 days of implantation, respectively. The fluorochrome signal from each sample approximates the infiltration of each cytokine and the respective intensity value is shown in the bar graphs for (c) and (d), respectively. e) ELISA analysis showed that the concentration of IL-17 and TNF- $\alpha$  infiltrated into each hydrogel after 3 and 7 days were significantly lower than that of ACS as the control. Scale bars: a,c) 100  $\mu$ m. Each error bar represents the standard deviation ( $n = 7$ , seven independent specimens were tested in each group.); NS = not significant; \*  $P < 0.05$ . Two-way (time  $\times$  material) ANOVA test was utilized to compare and analyze the obtained data.

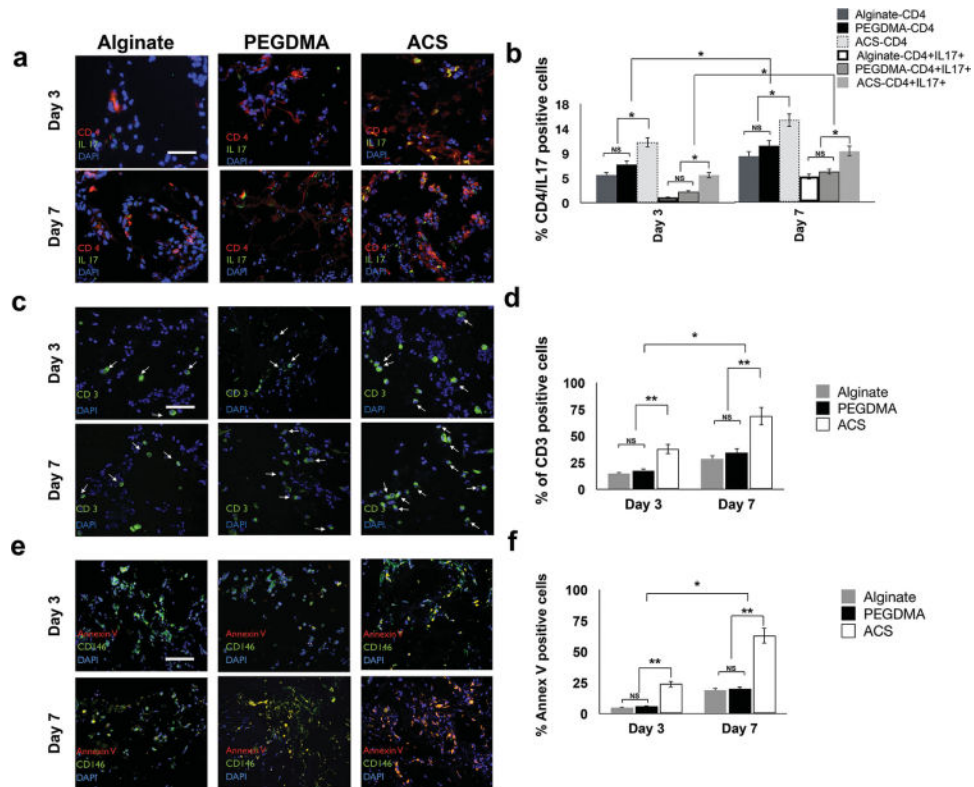


**Figure 3.**

Encapsulating hydrogel reduces apoptosis of implanted BMMSCs via reduction of pro-inflammatory T-lymphocyte penetration leading. Encapsulated BMMSCs ( $2 \times 10^6$  cells  $\text{mL}^{-1}$  of RGD-coupled alginate as well as PEGDMA) were subcutaneously implanted into WT mice. After 3 or 7 days, the specimens were retrieved and the presence of Th17 (CD4+, IL-17+) cells, Pan-T (CD3+) cells, and cells expressing Annexin V-PE (apoptosis marker) and CD-146 (MSC marker) within the microspheres were detected by immunofluorescence labeling with their respective antibody and counterstaining with DAPI using CLSM. a,b) CD4- and IL-17 double immunofluorescence staining showed reduced Th17 cell infiltration in alginate (or PEGDMA) hydrogel in comparison to the ACS group after 3 or 7 days of implantation in WT mice. c,d) Immunofluorescence staining showed decreased infiltration of CD3+ T lymphocytes in alginate (or PEGDMA) hydrogel in comparison to ACS matrix after 3 or 7 days of implantation (white arrows indicate CD3+ cells). e,f) CD146 and Annexin V double immunofluorescence staining showed reduced apoptosis of BMMSCs encapsulated in alginate (or PEGDMA) hydrogel compared to BMMSCs implanted with ACS as the carrier 3 or 7 days postimplantation in WT mice. No statistically significant difference was observed in any of the experiments between either of the used hydrogels. Scale bars: a), 200  $\mu\text{m}$ ; c, e), 100  $\mu\text{m}$ . Each error bar represents the standard deviation; \*  $P < 0.05$  and \*\*\*  $P < 0.001$ . Two-way (time  $\times$  material) ANOVA test was utilized to compare and analyze the obtained data.

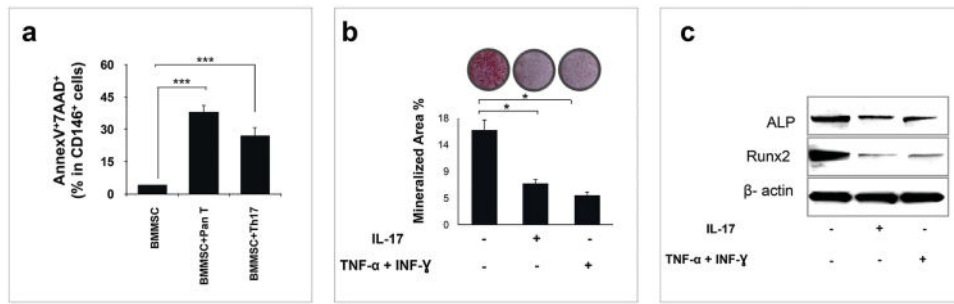


**Figure 4.**

Pro-inflammatory cytokines induce BMMSC apoptosis and reduce their osteogenic capacity.

a) The rate of MSC apoptosis using an Annexin V-PE apoptosis detection kit was performed

on  $0.2 \times 10^6$  BMMSCs cocultured separately with  $1 \times 10^6$  of either Pan-T or Th17 cells.

After 3 days of culture, FACS (fluorescence activated cell sorting) analysis showed

increased apoptosis of BMMSCs after pro-inflammatory T-cell coculture. b) The in vitro inhibitory effects of pro-inflammatory cytokines on osteogenic differentiation was shown by

BMMSCs ( $0.2 \times 10^6$ ) cultured under osteogenic conditions for 2 weeks with inflammatory cytokines [IL-17 ( $10 \text{ ng mL}^{-1}$ ), IFN- $\gamma$  ( $50 \text{ ng mL}^{-1}$ ), and TNF- $\alpha$  ( $5 \text{ ng mL}^{-1}$ )] added to the osteogenic culture medium every 3 days. Alizarin red staining revealed reduced mineralized nodule formation.

c) Western blot analysis showed that pro-inflammatory cytokine-treated BMMSCs expressed reduced levels of select osteogenic markers including RUNX2 and ALP.  $\beta$ -Actin was used as a protein loading control.

Each error bar represents the standard deviation; \*  $P < 0.05$ , and \*\*\*  $P < 0.001$ . Two-way (time  $\times$  material) ANOVA test was utilized to compare and analyze the obtained data.

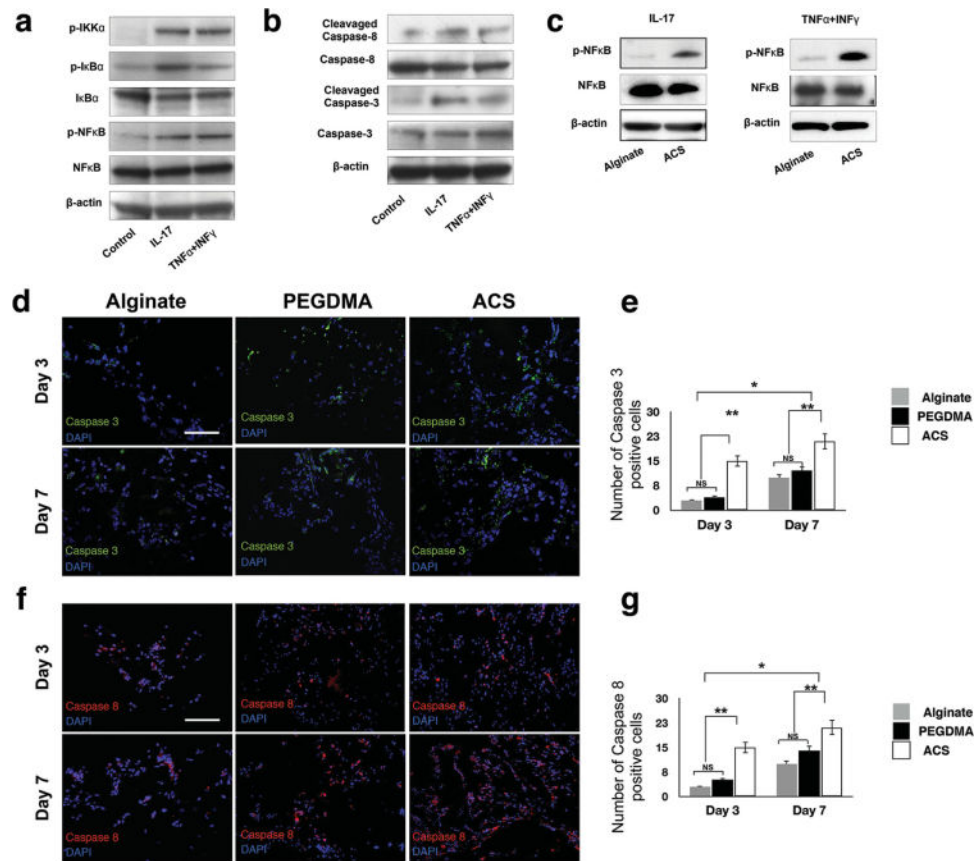


**Figure 5.**

Pro-inflammatory cytokines activated CASPASE-dependent apoptotic pathway through NF-κB cascades in BMMSCs. To confirm the deleterious effects of pro-inflammatory cytokines on MSC survival and dissect the molecular mechanism of action,  $0.5 \times 10^6$  BMMSCs were cocultured separately with IL-17 or with IFN- $\gamma$  in combination with TNF- $\alpha$  for 3 days. Pathway activation was analyzed through Western blotting for NF-κB, IKK $\beta$ , CASPASE-3, and CASPASE-8 antibodies. a) Western blot analysis revealed evidence for activated NF-κB cascades in BMMSCs after pro-inflammatory cytokine treatment compared to controls. b) Western blot analysis demonstrated more activated CASPASE-3 and CASPASE-8 in BMMSCs after pro-inflammatory cytokine treatment than in controls. c) BMMSCs ( $1 \times 10^6$ ) were encapsulated in alginate or seeded onto ACS, then cocultured with IL-17 or a combination of IFN- $\gamma$  with TNF- $\alpha$  for 3-days. Western blot analysis showed downregulation of apoptosis-related proteins CASPASE-3 and CASPASE-8 for BMMSCs encapsulated in alginate hydrogel in comparison to cells seeded on ACS. d,e) To corroborate these in vitro results in an in vivo environment, BMMSCs ( $2 \times 10^6$  cells mL $^{-1}$  alginate or PEGDMA) were subcutaneously implanted into WT mice. Immunofluorescence staining with antibodies against CASPASE-3 and CASPASE-8 of specimens retrieved at 3 or 7 days after implantation showed significantly higher CASPASE-3 expression in MSCs implanted in ACS compared to MSCs encapsulated in alginate or PEGDMA hydrogels. f,g) Immunofluorescence staining showed higher CASPASE-8 expression in MSCs grown on ACS in comparison to alginate or PEGDMA hydrogels after 3 or 7 days of implantation in

WT mice. Scale bars: d,f), 200  $\mu\text{m}$ . Each error bar represents the standard deviation; \*  $P < 0.05$ , and \*\*\*  $P < 0.001$ . Kruskal–Wallis test was utilized to compare and analyze the obtained data.



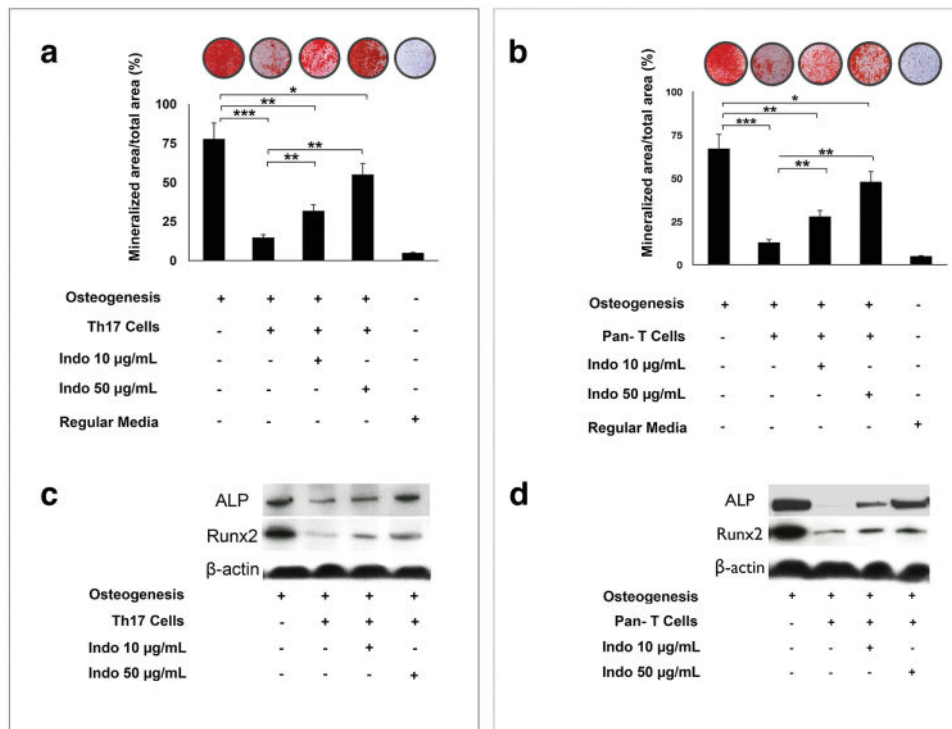


**Figure 6.**

Indomethacin treatment rescued bone regeneration ability of implanted BMMSCs in vitro. To test whether local administration of the anti-inflammatory drug indomethacin improves MSC-mediated bone regeneration,  $0.2 \times 10^6$  BMMSCs were cocultured under osteogenic culture conditions in the presence of either  $1 \times 10^6$  CD-3 activated T-lymphocytes or Th17 lymphocytes for 2 days. Indomethacin ( $10$  or  $50 \mu\text{g mL}^{-1}$ ) was added to the osteogenic differentiation media. After 2 weeks of treatment the samples were stained with Alizarin red for detection of calcium deposits, and RUNX2 and ALP expression levels were assayed by Western blot. a) Indomethacin treatment improved osteogenesis of BMMSCs cocultured with Th17 cells under osteoinductive conditions. b) Indomethacin treatment rescued osteogenesis of BMMSCs cocultured with CD-3 activated T lymphocytes under osteoinductive conditions. c) BMMSCs treated with CD-3 activated T-lymphocytes or Th17 lymphocytes expressed reduced levels of the osteogenic markers RUNX2 and ALP, while indomethacin treatment significantly increased the expression of the same osteogenic markers, as assessed by Western blot analysis. Each error bar represents the standard deviation ( $n = 7$ , seven independent specimens were tested in each group); \*  $P < 0.05$ , \*\*  $P < 0.01$ , and \*\*\*  $P < 0.001$ . ANOVA test was utilized to compare and analyze the obtained data.

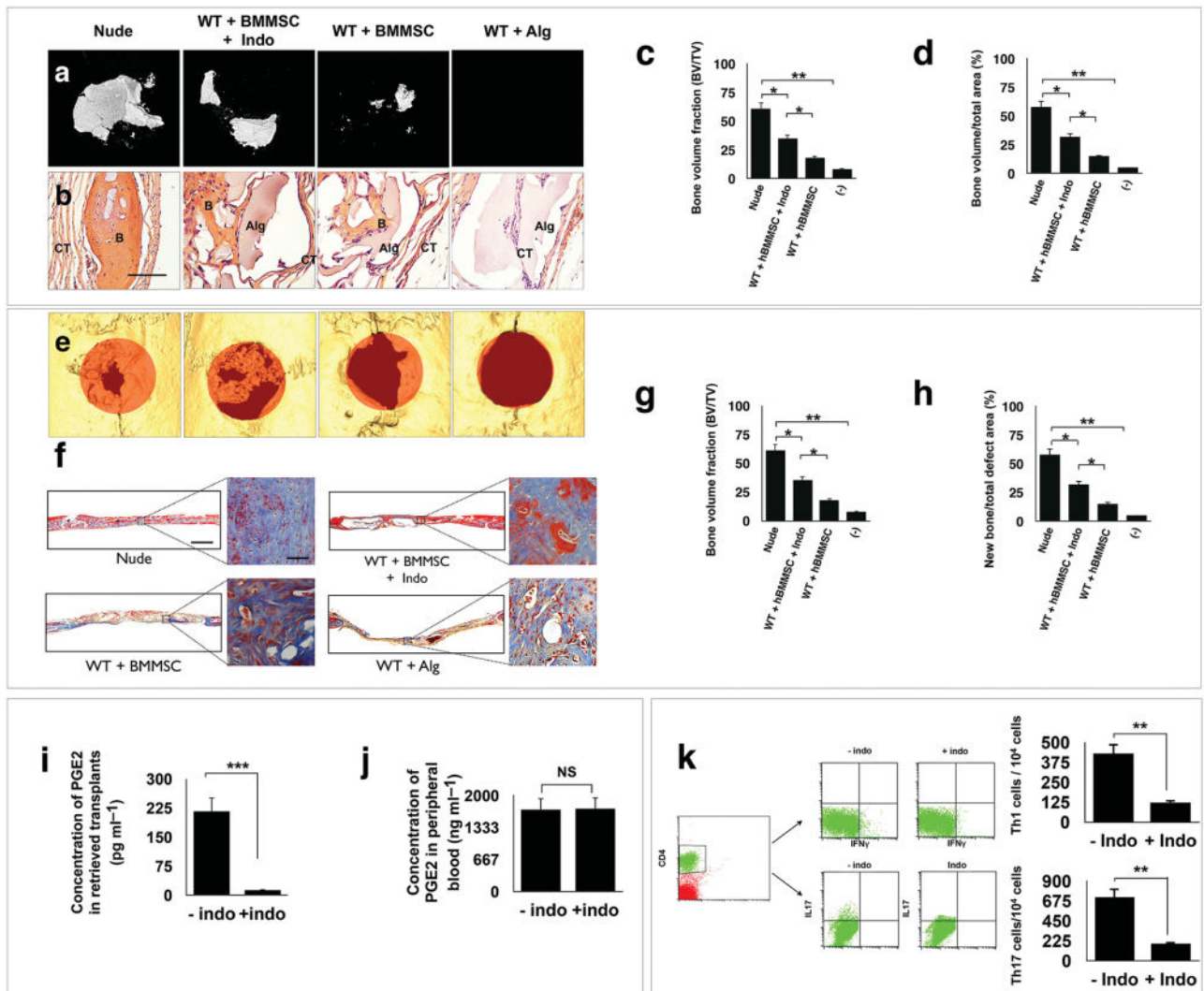


**Figure 7.**

Indomethacin treatment rescued bone regeneration ability of implanted BMMSCs in mouse model. To corroborate the in vitro effects of indomethacin in vivo,  $4 \times 10^6$  BMMSCs were encapsulated in alginate hydrogel containing indomethacin ( $50 \mu\text{g mL}^{-1}$ ) and implanted subcutaneously or in a 5 mm diameter calvarial defect in WT mice. a,b) Implantation of BMMSCs encapsulated in alginate hydrogel loaded with indomethacin ( $50 \mu\text{g mL}^{-1}$ ) revealed increased bone regeneration at the ectopic site, shown by micro-CT and histologic analysis (c,d). e,f) Increased bone regeneration was observed at the calvarial defect, compared to groups that received BMMSC-alginate constructs without indomethacin or alginate alone. g) Bone volume fraction (BV/TV) was assessed by micro-CT images in e,h) bone volume/total area identified by histomorphometric analysis of the retrieved specimens based on (f). i) ELISA analysis showing the reduced concentration of prostaglandin E2 (PGE2) in subcutaneous transplants in WT mice in presence of indomethacin. However, no difference was found in the levels of PEG2 in peripheral blood in presence or absence of indomethacin (j). k) Multicolor flow cytometric analysis showed significant decrease in the number of Th1 and Th17 cells in the retrieved subcutaneous specimens in the presence of

indomethacin. Alg = alginate; B = Bone; CT = connective tissue. Scale bars: a), 200  $\mu\text{m}$ ; g), 500  $\mu\text{m}$  (high mag), 50  $\mu\text{m}$  (low mag). Each error bar represents the standard deviation; \*  $P < 0.05$ , \*\*  $P < 0.01$ , and \*\*\*  $P < 0.001$ . Kruskal–Wallis test and Mann–Whitney  $U$  test were utilized for (a–h) and (i–j), respectively.  $T$ -test was used for k) to compare and analyze the obtained data.